Neuropsychopharmacology (2007) 32, 2249–2259

www.neuropsychopharmacology.org

Striatal Adenosine A_{2A} and Cannabinoid CB_1 Receptors Form Functional Heteromeric Complexes that Mediate the Motor Effects of Cannabinoids

Paulina Carriba[1], Oskar Ortiz[2], Kshitij Patkar[3], Zuzana Justinova[4,5], Jessica Stroik[4], Andrea Themann[6], Christa Müller[6], Anima S Woods[3], Bruce T Hope[7], Francisco Ciruela[1], Vicent Casadó[1], Enric I Canela[1], Carme Lluis[1], Steven R Goldberg[4], Rosario Moratalla[2,8], Rafael Franco[1,8] and Sergi Ferré*[,4,8]

[1]Department of Biochemistry and Molecular Biology, University of Barcelona, Barcelona, Spain; [2]Instituto Cajal, Consejo Superior de Investigaciones Científicas, Madrid, Spain; [3]Proteomics Laboratory, Department of Health and Human Services, National Institute on Drug Abuse, Intramural Research Program, National Institutes of Health, Baltimore, MD, USA; [4]Preclinical Pharmacology Section, Department of Health and Human Services, National Institute on Drug Abuse, Intramural Research Program, National Institutes of Health, Baltimore, MD, USA; [5]Department of Psychiatry, Maryland Psychiatric Research Center, University of Maryland School of Medicine, Baltimore, MD, USA; [6]Pharmaceutical Institute, University of Bonn, Bonn, Germany; [7]Neurobiology of Relapse Section, Department of Health and Human Services, National Institute on Drug Abuse, Intramural Research Program, National Institutes of Health, Baltimore, MD, USA

The mechanism of action responsible for the motor depressant effects of cannabinoids, which operate through centrally expressed cannabinoid CB_1 receptors, is still a matter of debate. In the present study, we report that CB_1 and adenosine A_{2A} receptors form heteromeric complexes in co-transfected HEK-293T cells and rat striatum, where they colocalize in fibrilar structures. In a human neuroblastoma cell line, CB_1 receptor signaling was found to be completely dependent on A_{2A} receptor activation. Accordingly, blockade of A_{2A} receptors counteracted the motor depressant effects produced by the intrastriatal administration of a cannabinoid CB_1 receptor agonist. These biochemical and behavioral findings demonstrate that the profound motor effects of cannabinoids depend on physical and functional interactions between striatal A_{2A} and CB_1 receptors.
Neuropsychopharmacology (2007) **32,** 2249–2259; doi:10.1038/sj.npp.1301375; published online 14 March 2007

Keywords: adenosine A_{2A} receptor; cannabinoid CB_1 receptor; receptor heteromerization; striatum; cyclic AMP; motor activity

INTRODUCTION

Activation of cannabinoid CB_1 receptors mediates most central effects of cannabinoids, such as Δ^9-tetrahydrocannabinol (THC), the main psychoactive ingredient of marihuana. One of the most salient effects of CB_1 receptor activation is motor depression, which is related to the significant modulatory role played by endocannabinoids in the basal ganglia (Gough and Olley, 1978; Ledent *et al*, 1999; Sanudo-Pena *et al*, 1999; van der Stelt and Di Marzo, 2003). CB_1 receptors are abundantly expressed in different structures of the basal ganglia, including the striatum (Herkenham *et al*, 1991). In the striatum, CB_1 receptors are localized in both types of GABAergic efferent neurons, enkephalinergic and dynorphinergic (Hohmann and Herkenham, 2000; Fusco *et al*, 2004), which constitute more than 90% of the striatal neuronal population (Gerfen, 2004). Furthermore, striatal CB_1 receptors are localized in parvalbumin-expressing GABAergic interneurons (Hohmann and Herkenham, 2000; Fusco *et al*, 2004) and presynaptically in glutamatergic and GABAergic terminals (Rodriguez *et al*, 2001; Kofalvi *et al*, 2005).

Similar to endocannabinoids, the neuromodulator adenosine plays a very important integrative role in striatal function (Ferré *et al*, 1997, 2005). Adenosine A_{2A} receptors are more concentrated in the striatum than anywhere else in the brain and they are strategically located, both pre- and postsynaptically, to modulate glutamatergic neurotransmission in GABAergic enkephalinergic neurons (Hettinger *et al*, 2001; Ferré *et al*, 2005; Ciruela *et al*, 2006). In the present study, we found that A_{2A} and CB_1 receptors co-immunoprecipitate from extracts of rat striatum, where they colocalize in fibrilar structures. In co-transfected mammalian cells we demonstrated that both receptors form direct physical interactions, that is A_{2A}–CB_1 receptor heteromers.

*Correspondence: Dr S Ferré, Preclinical Pharmacology Section, Department of Health and Human Services, National Institute on Drug Abuse, IRP, NIH, 5500 Nathan Shock Dr, Baltimore, MD 21224, USA, E-mail: sferre@intra.nida.nih.gov
[8]These authors contributed equally to this work.
Received 3 August 2006; revised 18 January 2007; accepted 19 January 2007

At a functional level, we also demonstrated that CB_1 receptor function is dependent on A_{2A} receptor activation both *in vitro* and *in vivo*. Thus, activation of A_{2A} receptors was necessary for CB_1 receptor signaling in a human neuroblastoma cell line and blockade of A_{2A} receptors significantly decreased the motor depressant effects of the central administration of the synthetic cannabinoid receptor agonist WIN 55 212-2 into the rat striatum.

MATERIALS AND METHODS

Immunohistochemistry

Adult male C57BL/6 wild type, A_{2A} receptor KO and CB_1 receptor KO mice, weighing 25–30 g, and adult male Wistar rats, weighing 250–300 g (Instituto Cajal, CSIC, Madrid, Spain) were used. Mice were only used to validate the antibodies to be applied in the immunohistochemical confocal experiments in the rat brain. The rat was the target animal species, as it was the most suitable to study the behavioral effects of intrastriatal administration of cannabinoid agonists. A_{2A} receptor KO and CB_1 receptor KO mice were generated as described elsewhere (Ledent *et al*, 1999; Chen *et al*, 1999). All animals used in a given experiment originated from the same breeding series, and were matched for age and weight. Mice were housed in groups of 4–5 per cage in clear plastic cages and maintained in a temperature- (22°C) and humidity-controlled room on a 12 h light–dark schedule with food and water provided *ad libitum*. The maintenance of the animals, as well as the experimental procedures, followed the guidelines from European Union Council Directive 86/609/EEC. All efforts were made to minimize the number of animals used and their suffering. The experimental protocols involving animals were approved by the local (CSIC) ethic committee. Animals were anesthetized by an intraperitoneal (i.p.) administration of pentobarbital (Lab Normon, Madrid, Spain) and perfused by means of a cannula introduced into the ascending aorta through the left ventricle. The vascular network was first washed of blood with saline solution (0.9% NaCl), followed by fixation with 4% paraformaldehyde in phosphate buffer (PB, 0.1 M, pH 7.4). The brains were then extracted and postfixed by immersion in the same fixative for 12–24 h at 4°C. Thereafter they were washed in two to three changes of PB 0.1 M and then cut with a vibrating blade microtome into 30-μm-thick coronal serial sections. Single- and double-labeling immunocytochemical techniques were employed for the detection of the antigens in free-floating sections. Adjacent serial sections of the same brains where the primary antibodies were omitted were analyzed to discriminate nonspecific staining. The absence of signal in sections from single CB_1 and A_{2A} KO mice showed the specificity of the primary antibodies used (see Figure 1). Sections were washed with three changes of PBT (PB 0.1 M, pH 7.4, containing 0.3% of Triton X-100), followed by a blocking solution (PBT containing 5% normal donkey serum). The primary antibodies were diluted in this blocking solution (1 : 250 for the CB_1 receptor and 1 : 500 for the A_{2A}). CB_1 receptor antibody was a rabbit polyclonal antiserum raised against a synthetic peptide corresponding to the first 14 amino acids on the amino terminus of the sequence for the rat receptor (Sigma, Saint Luis, MO, USA),

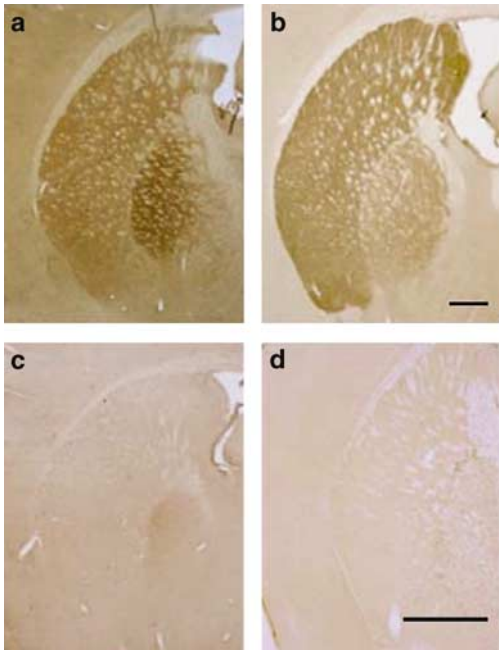

Figure 1 A_{2A} and CB_1 receptors expression in the mouse striatum. Microphotographs of coronal sections of mouse striatopallidal complex illustrating the distribution of CB_1 and A_{2A} receptors. Sections were immunohistochemically stained with anti-CB_1 or anti-A_{2A} receptor antibody as described in Materials and methods. (a) and (b) show CB_1 (a) and A_{2A} (b) receptor distribution in wild-type mouse. For negative controls, immunolocalization of CB_1 (c) or A_{2A} (d) receptors was attempted in samples from, respectively, CB1 or A_{2A} single KO mice; the absence of signal in these samples demonstrates the specificity of the antibodies.

and has been described and characterized elsewhere (Howlett *et al*, 1998). A_{2A} receptor antibody was a mouse monoclonal antibody (05-717, Upstate, Lake placid, NY, USA). Sections were incubated for 3 and 1 days with the CB_1 receptor and the A_{2A} antibody, respectively, under continuous shaking at 4°C. Then, sections were washed several times in PBT and incubated for 90 min with a donkey biotinylated anti-rabbit secondary antibody (1 : 500) for the CB_1 receptor (RPN1004V1, Amersham Biosciences, Buckinghamshire, UK) and with a donkey anti-mouse secondary antibody conjugated to Alexa Fluor 594 (red fluorescence) (1 : 500) (Molecular Probes, Leiden, The Netherlands) for the A_{2A} receptor. In order to determine the presence of the CB_1 receptor, sections were washed several times in PBT and incubated for 1 h with Streptavidine conjugated to Alexa Fluor 488 (green fluorescence) (1 : 3000) (Molecular Probes). Finally, sections were washed in PB repeatedly and mounted using Polyvinyl alcohol mounting medium plus 1,4-diazobicyclo[2,2,2]-octane (antifading) (Sigma). Images of the sections were obtained by confocal microscopy.

Co-immunoprecipitation

Male Sprague–Dawley rats (Charles River Laboratory, Wilmington, MA, USA) weighing 300–350 g were used in co-immunoprecipitation experiments. Animals were maintained in accordance with guidelines of the Institutional Care and Use Committee of the Intramural Research Program, National Institute on Drug Abuse, NIH. Rats were

killed with an overdose of Equithesin (NIDA Pharmacy, Baltimore, MD, USA). The striatal tissue was dissected on ice and the tissue was homogenized in 50 mM Tris-HCl, 5 mM EDTA, and Complete Mini peptidase inhibitors (Roche Applied Sciences, Basel, Switzerland), and centrifuged for 30 min at 20 000*g* at 4°C. Pellets were resuspended in solubilization buffer (10 mM Tris-HCl, 1 mM EDTA, 1% CHAPS, and the peptidase inhibitors) and centrifuged for 1 h at 150 000*g* at 4°C. Protein concentration in the supernatant was assayed using the bichinconinic acid assay (Pierce Biotechnology, Rockford, IL, USA). The specific receptor antibodies used were anti-A_{2A} receptor rabbit polyclonal IgG (VCR1) (Hillion *et al*, 2001) and anti-CB_1 receptor rabbit polyclonal IgG (PA1-745; Affinity BioReagents, Golden, CO, USA). The selectivity of both antibodies has been previously characterized (Hillion *et al*, 2001; Twitchell *et al*, 1997). The antibody against the cAMP response element binding protein (Cell Signaling Technologies, Beverly, MA, USA) was used as a control antibody. All three antibodies were immobilized on AminoLink Plus Coupling Gel using the Seize Primary Mammalian Immunoprecipitation Kit from Pierce Biotechnology. The solubilized striatal tissue was incubated with the immobilized antibody support and the receptors were co-immunoprecipitated using the immobilized antibodies. The beads were washed repeatedly with buffers containing varying concentrations of sodium chloride and Tris to wash away any nonspecifically bound proteins to the beads. The immunoprecipitated receptors were eluted off the immobilized antibody support using 2% SDS solution and the antibody support was regenerated for reuse. The immunoprecipitates were mixed with the loading buffer and resolved by SDS-PAGE. Western blots were performed with anti-CB_1 receptor antibodies.

Cell Cultures and Transfections

HEK-293T cells were used to demonstrate heteromerization of co-transfected constructs of A_{2A} and CB_1 receptors (A_{2A}-*Rluc* and CB_1-YFP) with bioluminescence resonance energy transfer (BRET) experiments. The human neuroblastoma cell line SH-SY5Y was used to investigate whether there is functional A_{2A}–CB_1 receptor cross-talk, as this cell line has been reported to constitutively express functional A_{2A} and CB_1 receptors (Salim *et al*, 2000; Hillion *et al*, 2001; Klegeris *et al*, 2003). HEK-293T cells were grown in Dulbecco's modified Eagle's medium (DMEM) (Gibco, Paisley, Scotland, UK) supplemented with 2 mM L-glutamine, 100 UI/ml penicillin/streptomycin, and 5% (v/v) heat-inactivated fetal bovine serum (FBS) (all supplements were from Invitrogen, Paisley, Scotland, UK). The SH-SY5Y neuroblastoma cell line was grown in DMEM (Gibco) supplemented with 2 mM L-glutamine, 100 UI/ml penicillin/streptomycin, 1 mM sodium pyruvate, and 10% (v/v) heat-inactivated FBS. Cells were maintained at 37°C in an atmosphere of 5% CO_2, and were passaged when they were 80–90% confluent, twice a week. Human A_{2A} receptor cDNA without its stop codon was amplified using sense and antisense primers harboring unique *Eco*RI and *Bam*HI sites. The fragment was then subcloned to be in-frame with *Rluc* into the *Eco*RI and *Bam*HI restriction sites of a *Renilla luciferase* expressing vector (pcDNA 3.1-*Rluc*) yielding the A_{2A}-*Rluc* construct. Human CB_1 receptor cDNA without its stop codon was amplified using sense and antisense primers harboring unique *Bam*HI and *Eco*RI sites. The fragment was then subcloned to be in-frame with EYFP into the *Bam*HI and *Eco*RI restrictions sites of a multiple cloning site of pEYFP-N1 (enhanced yellow variant of GFP; Clontech, Heidelberg, Germany) yielding the CB_1-YFP construct. Both constructs express *Rluc* or EYFP on the C-terminal ends of the receptor. Functionality of the constructs transiently transfected in HEK 239T cells was tested by ERK1/2 phosphorilation assay (data not show). HEK-293T cells growing in six-well dishes were transiently transfected with 12 μg of DNA by PolyEthylenImine (PEI; Sigma, Steinheim, Germany) method. Various amounts of DNA for the construct CB_1-YFP were used with 2 μg of A_{2A}-*Rluc*. To maintain the ratio of DNA in co-transfections, the empty vector, pcDNA 3.1, was used to equilibrate the amount of total DNA transfected. For transient transfections, cells were incubated with a mix containing constructs DNA, 5.47 mM nitrogen residues of PEI, and 150 mM NaCl in a serum-starved medium. After 4 h, medium was changed to a fresh complete medium. BRET immunolabeling and BRET experiments were performed 48 h after transfection.

Immunocytochemistry

SH-SY5Y cells were grown on glass coverslips coated with poly-L-lysine (Sigma). At 60% confluence, cells were rinsed with PBS, fixed in 4% paraformaldehyde for 15 min, and washed with PBS containing 20 mM glycine. Cells were permeabilized with PBS containing 20 mM glycine, 1% bovine serum albumin (BSA) (buffer A), and 0.05% Triton X-100 during 5 min, and were blocked with buffer A for 1 h at room temperature. Cells were labeled for 1 h with mouse monoclonal anti-A_{2A} receptor antibody (05-717, Upstate, Lake Placid, NY, USA). Then, were washed and stained for 1 h with cyanine 3-conjugated affinity purified donkey anti-mouse IgG (Jackson ImmunoResearch, West Grove, USA) and with cyanine 5-conjugated rabbit anti-CB_1 receptor antibody (Affinity Bioreagents), labelled in our laboratory using FluoroLink Cy5 reactive dye pack (Amersham Biosciences). The coverslips were rinsed for 30 min in buffer A and mounted with Vectashield Mounting Medium for Fluorescence (Vector Laboratories Inc. Burlingame, CA, USA). Microscopic observations were made in Olympus FV 300 confocal scanning laser microscope (Leica Lasertechnik, Leica Microsystems, Mannheim, Germany). Expression of the A_{2A}-*Rluc* and CB_1-YFP constructs were also tested by confocal microscopy. HEK-293T cells transiently transfected with the cDNA of fusion proteins were grown on glass coverslips coated with poly-L-lysine (Sigma), 48 h after transfections, rinsed with PBS, and fixed in 4% paraformaldehyde for 15 min. To detect the expression of the A_{2A}-*Rluc* construct the same protocol as described above was used, whereas to detect the CB_1-YFP construct its fluorescent properties were used. Coverslips were washed with buffer A and mounted as describe above.

BRET Experiments

At 48 h after transfection, cells were rapidly washed twice in HBSS with 10 mM glucose, detached, and resuspended in

the same buffer containing 1 mM EDTA. To control the cell number, sample protein concentration was determined using a Bradford assay kit (Bio-Rad, Munich, Germany) using BSA dilutions as standards. To quantify fluorescence of CB_1-YFP, cells (20 μg protein) were distributed in duplicated 96-well microplates (black plates with a transparent bottom) and read in a Fluostar Optima Fluorimeter (BMG Labtechnologies, Offenburg, Germany) equipped with a high-energy xenon flash lamp, using a 10-nm bandwidth excitation filter at 485 nm. YFP fluorescence was the fluorescence of the sample minus the fluorescence of cells not expressing CB_1-YFP. For BRET measurement, the equivalent of 20 μg of cell suspension were distributed in triplicates in 96-well microplates (Corning 3600, white plates with white bottom) and 5 μM coelenterazine H (Molecular Probes, Eugene, OR, USA) was added. After 1 min, the readings were collected using a Mithras LB 940 (Berthold Technologies, DLReady, Germany) that allows the integration of the signals detected in the filter at 485 nm (440–500 nm) and the 530 nm (510–590 nm). To quantify luminescence of *Rluc*, readings were taken after 10 min of adding 5 μm coelenterazine H. The BRET signal was determined by calculating the ratio of the light emitted by YFP (510–590 nm) over the light emitted by the *Rluc* (440–500 nm). The net BRET values were obtained by subtracting the BRET background signal detected when *Rluc*-tagged construct was expressed alone. Curves were fitted using a nonlinear regression and one-phase exponential association fit equation (GraphPad Prism, San Diego, CA, USA).

RT-PCR

Total cellular RNA was isolated from confluent cultures of SH-SY5Y cells using QuickPrep Total RNA Extraction Kit (Amersham Biosciences) following the manufacturer's instructions. For the RT-PCR assay, 1 μg of total RNA was reverse transcribed by random priming using M-MLV Reverse Transcriptase, RNase H Minus, and Point Mutant, following the protocol of two-step RT-PCR provide by data sheet of Promega (Promega, Madison, WI, USA). The resulting single-stranded cDNA was used to perform PCR amplification for CB_1 receptor, A_{2A} receptor, and tubulin as an internal control of PCR technique. Samples, composed by master mix, that includes *Taq* DNA Polymerase, dNTPs, $MgCl_2$, and reaction buffers at optimal concentrations for efficient amplification of DNA templates (Promega), primers and cDNA, were denatured at 95°C for 2 min, and then subjected to 35 cycles of 95°C for 1 min, 58°C to annealing CB_1 receptor primers, and 60°C to annealing A_{2A} receptor primers during 1 min and extensions of 2 min at 72°C, with a 10 min extension at 72°C during the last cycle on a Techne thermal cycler. The primers used to amplify the human CB_1 receptor gene were 5′-TGGGCAGCCTGTTCCT CAC-3′ (forward) and 5′-CATGCGGGCTTGGTC-3′ (reverse). To amplify the human A_{2A} receptor, the primers used were 5′-CATCCCCTTTGCCATCACCATCAG-3′ (forward) and 5′-GTAGGGGCAGCCAGCAGAGG-3′ (reverse). To amplify tubulin, the primers used were 5′-CATG ATGGCCGCCTGCGACC-3′ (forward) and 5′-CCTGGATGG CCGTGCTGTTGC-3′ (reverse). The expected size of the amplicons was 400 bp for the CB_1 receptor, 571 bp for A_{2A} receptor, and 232 bp for tubulin. The PCR products were electrophoresed on a 1% agarose gel. RNA without reverse transcriptions did not yield any amplicons, indicating that there was no genomic DNA contamination.

cAMP Determination

The accumulation of cAMP was measured with Cyclic AMP (^{3}H) Assay System (Amersham Biosciences) as described in the manual from the manufacturer. About 80% confluent SH-SY5Y cells were serum-starved during 12–16 h supplemented or not with 2 UI/ml of adenosine deaminase (ADA; Roche, Basel, Switzerland) and the medium was replaced for the same fresh medium immediately before 50 μM Zardaverine addition as phosphodiesterase inhibitor. After 15 min at 37°C, the A_{2A} receptor antagonist 4-(2-[7-amino-2-(2-furyl[1,2,4]-triazolo[2,3-a[1,3,5]triazin-5-yl-aminoethyl)-phenol (ZM241385; 1 μM) (Cunha *et al*, 1997) or the CB_1 receptor antagonist *N*-(piperidin)-1-yl)-5-(4-iodophenyl)-1-(2,4-dichlorophenyl)-4-methyl-1*H*-pyrazole-3-carboxamide (AM251; 1 μM) (Lan *et al*, 1999) were added and incubated 5 min before agonist addition. The A_{2A} receptor agonist 2-*p*-(2-carboxyethyl)phenethylamino-5′-*N*-ethylcarboxamidoadenosine (CGS 21680, 200 nM) (Karcz-Kubicha *et al*, 2003) and the selective CB_1 receptor agonist arachidonyl-2-chloroethylamide (ACEA, 50 nM) (Hillard *et al*, 1999) were added with or without 10 μM forskolin and incubated for 30 min at 37°C. CGS 21680 and forskolin were from Sigma, the rest of reagents were from Tocris, Bristol, UK. CGS 21680 and ZM241385 were initially dissolved in DMSO (concentration of DMSO in the final dilution was $<0.01\%$). ACEA and AM251 were initially diluted in ethanol (concentration of ethanol in the final dilution was $<0.01\%$). One-way ANOVA followed by Newman–Keuls *post hoc* test was used for statistical comparisons.

Motor Activity

Male Sprague–Dawley rats (Charles River Laboratory) weighing 300–350 g were used in the motor activity experiments. The animals were stereotaxically implanted with stainless-steel guide cannulae (22 G, Plastic ONE, Roanoke, VA, USA) in the right and left dorsal striatum under Equithesin (NIDA Pharmacy) anesthesia (coordinates respect to bregma: A 0.0, L ± 3.5, V −5.0). Guide cannulae were fixed with dental acrylic and stainless-steel screws to the skull surface. Stainless-steel stylets were inserted into the cannulae to prevent occlusion. A recovery period of 3 or 4 days was allowed before testing. For intrastriatal administration, injection needles (28 G) extending 0.5 mm below the guide were inserted into the cannulae. The cannabinoid receptor agonist *R*-(+)-[2,3-dihydro-5-methyl-3-(4-morpholinylmethyl) pyrrolo-[1,2,3-d,e]-1,4-benzoxazin-6-yl]-1-naphthalenyl-methanone mesylate (WIN 55 212–2; 40 μg dissolved in 5% Tween 80-saline) (Felder *et al*, 1995; Hillard *et al*, 1999) or vehicle (5% Tween 80-saline) was administered intrastriatally at a rate of 0.5 μl/min by means of a microdrive pump (final injection volume: 1 μl). The dose and rate of administration of WIN 55 212–2 was chosen according to pilot experiments and previously published studies on motor depressant effects induced by intrastriatal administration of THC (Gough and Olley, 1978). The needle was then left in place for an

additional 2 min before being replaced by the stylet. About 20 min before the intrastriatal administration, saline, the CB_1 receptor antagonists AM251 (3 mg/kg), and *N*-(piperidin-1-yl)-5-(4-chlorophenyl)-1-(2,4-dichlorophenyl)-4-methyl-1*H*-pyrazole-3-carboximide hydrochloride (SR141716A; 3 mg/kg) (Felder *et al*, 1995) or the A_{2A} receptor antagonist 3-(3-hydroxypropyl)-8-(m-methoxystyryl)-7-methyl-1-propargylxanthine phosphate disodium (MSX-3; 3 mg/kg) (Karcz-Kubicha *et al*, 2003; Sauer *et al*, 2000) were administered i.p. (1 ml/kg for SR141716A and MSX-3 and 2 ml/kg for AM251). SR141716A and AM251 were dissolved in a vehicle of 2% ethanol, 2% Tween 80, and saline and MSX-3 was dissolved in saline with a few drops of 0.1 N NaOH (final pH: 7.4). SR141716A and AM251 were from Sigma and MSX-3 was synthesized at the Pharmaceutical Institute, University of Bonn, Germany. About 20 min after the intrastriatal administration, the animals were placed in a Columbus Instruments Auto-Track system (Coulbourn Instruments, Lehigh Valley, PA) to quantify motor activity (ambulatory distance and stereotypies). Motor activity was recorded during the first 20 min (maximal period of exploratory activity) in 5-min intervals. The average of the motor activity recordings obtained during the first four 5-min intervals was used to analyze differences between the differently treated groups of animals. One-way ANOVA with Dunnett's multiple comparison tests were used for statistical analysis. At the end of the experiment, rats were killed with an overdose of Equithesin, the brain was removed and placed in a 10% formaldehyde solution, and coronal sections were cut to verify cannulae location.

Competition Binding Assays

Frozen rat brains obtained from Pel Freez, Rogers, AR, USA, were dissected to obtain cortical and striatal membrane preparations as described elsewhere (Sauer *et al*, 2000). ZM241385 and MSX-2 and its phosphate pro-drug MSX-3 were investigated in competition experiments versus the CB_1 receptor agonist [^{3}H]CP55 940 (158 Ci/mmol; Amersham, Rossendaal, The Netherlands). MSX-2 was tested as it is the dephosphorylated active compound of MSX-3, which cannot be converted to MSX-2 in *in vitro* experiments. Stock solutions of the compounds were prepared in DMSO. Final DMSO concentrations in the assays did not exceed 2.5%. Competition experiments were performed using 0.1 nM [^{3}H]CP55 940 at room temperature in plastic tubes with rat brain cortical or striatal membranes (50 μg of protein per tube) in 1 ml (final volume) of buffer solution (50 mM Tris-HCl, 3 mM $MgCl_2$, 0.1% BSA, pH 7.4). Nonspecific binding was determined in the presence of 10 μM of CP55 940. After 2 h the incubation was stopped, solutions were rapidly filtered through GF/C glass fiber filters on a 24-Brandell cell harvester, and washed three times with 3 ml each of ice-cold washing buffer solution (50 mM Tris-HCl, 0.1% BSA, pH 7.4). Filters were dried, scintillation cocktail (Ultima Gold, Perkin-Elmer) was added, and radioactivity was measured using a liquid scintillation counter (Tri-Carb 2900TR, Packard). Three independent experiments were performed, each in triplicate. Protein concentrations were determined by the method of Lowry.

RESULTS

Colocalization and Co-immunoprecipitation of A_{2A} and CB_1 Receptors in the Rat Striatum

Immunohistochemical experiments were carried out to test whether A_{2A} and CB_1 receptors are coexpressed in striatal neurons. Immunological staining of coronal sections of mouse striatopallidal complex with the anti-CB_1 or the anti-A_{2A} receptor antibodies showed a predominant labeling of A_{2A} and CB_1 receptors in the striatum and globus pallidus (Figures 1a and b). CB_1 receptor immunostaining was moderate in the striatum and strongest in the pallidum, whereas A_{2A} receptors were mainly localized in the striatum. The labeling profile of the two antibodies was very similar, tagging primarily the neuropil and avoiding the neuronal cell bodies. Similar results were obtained using coronal sections of rat brain (results not shown), which agrees with previous reports (Herkenham *et al*, 1991; Hettinger *et al*, 2001). No immunostaining was found in samples from genetically modified CB_1 or A_{2A} knockout mice (Figure 1c and d), which demonstrates the specificity of the primary antibodies.

Double immunofluorescence staining of coronal sections of rat striatum revealed a green fluorescent signal corresponding to CB_1 receptors and a red fluorescent signal corresponding to A_{2A} receptors, in fibrilar structures (Figure 2). Both labeled profiles had a dispersed appearance with clear contrast between the unlabeled cell bodies or fiber bundles (with no fluorescence signal) and the surrounding labeled neuropil. Thus, CB_1 or A_{2A} receptor-immunoreactive fibers had the appearance of a meshwork, indicative of striatal neuropil, perforated by unlabeled cell bodies (Figure 2a–f). This was clearly evident at a higher magnification, where sharply delineated cells bodies devoid of any of the two labels were observed, whereas cell membrane profiles were clearly labeled with both CB_1 and A_{2A} receptor antibodies (Figure 2g and h, respectively). Occasionally, primary dendrites were also labeled with the two antibodies (Figure 2g and 2h). Merging of the red and green images showed a strong colocalization (yellow signal) of CB_1 and A_{2A} receptors in the same striatal neurons (Figure 2c, f and i). A yellow fluorescent signal showed colocalization of CB_1 and A_{2A} receptors in approximately half of the total fibers expressing CB_1 receptors, and the presence of green (CB_1 receptor immunoreactivity) and absence of red (A_{2A} receptor immunoreactivity) signal in the merged images indicates that most A_{2A} receptors are colocalized with CB_1 receptors, but that there is a proportion of CB_1 receptors that does not colocalize with A_{2A} receptors (Figure 2c, f and i). This agrees with the more widespread localization of striatal CB_1 receptors compared to A_{2A} receptors (see Introduction). Overall, results shown in Figure 2 demonstrate that CB_1 and A_{2A} receptors are present in the same striatal neurons. It remains to be determined if striatal A_{2A} and CB_1 receptors are preferentially colocalized postsynaptically, in GABAergic enkephalinergic dendrites, or also presynaptically, in glutamatergic terminals, as positive immunoreactive fibrilar structures were compatible with both dentritic processes and nerve terminals.

To test for the existence of physical interactions between A_{2A} and CB_1 receptors in the striatum, co-immunoprecipitation experiments were performed. As shown in Figure 3, a

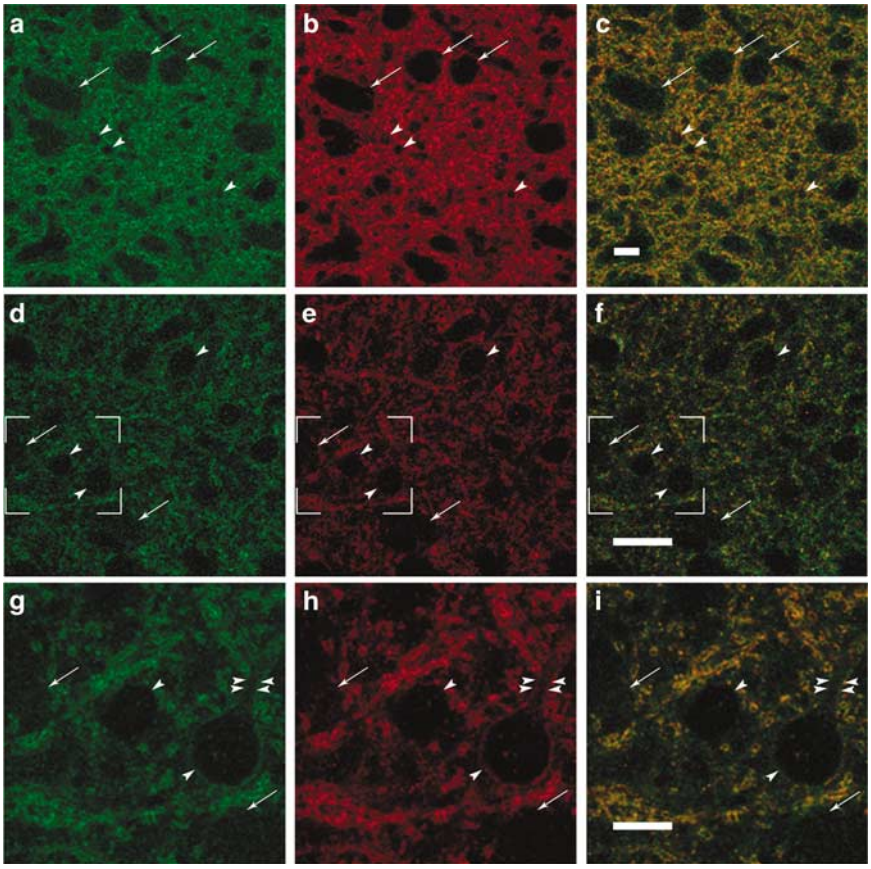

Figure 2 A_{2A} and CB_1 receptors colocalization in rat striatum. Coronal sections of rat striatum were processed for immunofluorescent histochemistry as described in Materials and methods (a, d, and g show CB_1 receptor staining as intense green fluorescent immunoreactive fibers. b, e, and h show A_{2A} receptor staining as red fluorescent immunoreactive fibers. c, f, and i correspond to merging of the green and red images, showing colocalization of CB_1 and A_{2A} receptors in approximately half of total fibres that express CB_1 receptors. g, h, and i are high-power microphotographs illustrating a detail indicated in d, e, and f, respectively (broken squares). Arrows and arrowheads indicate striatal fiber bundles and neurons, respectively. Double arrowheads indicate a primary dendrite. a, b, c, d, e, and f scale bars = 20 μm; f, h, and g scale bars = 40 μm.

predominant band at about 60 kDa, corresponding to the CB_1 receptor, could be observed in the lysate and in the immunoprecipitate obtained using either the CB_1 receptor antibody or the A_{2A} receptor antibody, but not when another antibody (anti-CREB) was used. These results indicate that heteromeric A_{2A}–CB_1 receptor complexes exist in the striatum. However, co-immunoprecipitation does not demonstrate the existence of true heteromers, as they do not discard the existence of intermediate proteins indirectly linking A_{2A} and CB_1 receptors.

A_{2A}–CB_1 Receptor Heteromerization in Living Cells

To demonstrate the existence of a direct physical interaction between A_{2A} and CB_1 receptors, BRET was carried out in living HEK293 cells transfected with cDNAs encoding the fusion proteins A_{2A}-*Rluc* (human A_{2A} receptor-*Renilla luciferase*) and CB_1-YFP (human CB_1 receptor-yellow fluorescent protein). After transfection, the receptors expression was high at the membrane level (Figure 4a). As energy transfer between two specifically interacting proteins has to reach a plateau, a saturable BRET curve was obtained for the A_{2A}-*Rluc*/CB_1-YFP pair when constant amounts of the cDNA for the *Rluc* construct were co-transfeted with increasing amounts of the plasmid cDNA for the YFP construct (Figure 4b). Maximum net BRET was 0.061 ± 0.004 (see Materials and methods) and $BRET_{50}$ was attained at a relatively low CB_1-YFP/A_{2A}-*Rluc* ratio (0.023 ± 0.003). As negative controls, no significant BRET was obtained in a mixture of cells transfected with A_{2A}-*Rluc* and cells transfected with CB_1-YFP or in cells co-transfected with A_{2A}-*Rluc* and with CD4-YFP (Figure 4b). These results indicate that the BRET signal obtained using A_{2A}-*Rluc*/CB_1-YFP was specifically due to A_{2A}–CB_1 receptor heteromerization. Treatment with either the A_{2A} receptor agonist CGS 21680 (200 nM), the CB_1 receptor agonist ACEA (100 nM), or both for 15 and 45 min did not induce any significant changes in the BRET signal, indicating that acute agonist treatment does not modify A_{2A}–CB_1 receptor heteromerization (data not shown).

Functional Cross-Talk between CB_1 and A_{2A} Receptors

The human neuroblastoma cell line SH-SY5Y with constitutive expression of A_{2A} and CB_1 receptors was used to investigate A_{2A}–CB_1 receptor cross-talk. The presence of A_{2A} and CB_1 receptors was confirmed by RT-PCR (Figure 5a), immunocytochemistry, and confocal laser

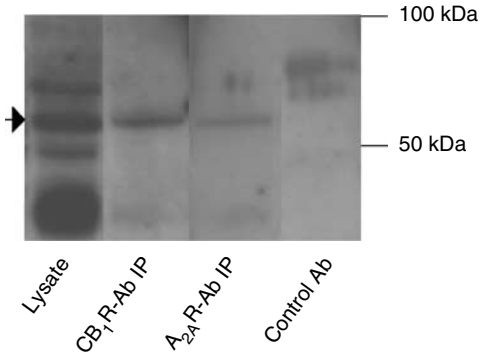

Figure 3 Co-immunoprecipitation of A_{2A} and CB_1 receptors from rat striatal membranes. Striatal membranes were prepared as described in Materials and methods and were processed for immunoprecipitation (see Materials and methods) with either anti-CB_1 receptor antibody (CB_1R-Ab-IP), anti-A_{2A} receptor antibody (A_{2A}R-Ab-IP), or anti-CREB antibody (for negative control). Immunoprecipitates were analyzed by SDS-PAGE and immunoblotted with the anti-CB_1 antibody. The arrow indicates the position of the band corresponding to the CB_1 receptor (about 60 kDa).

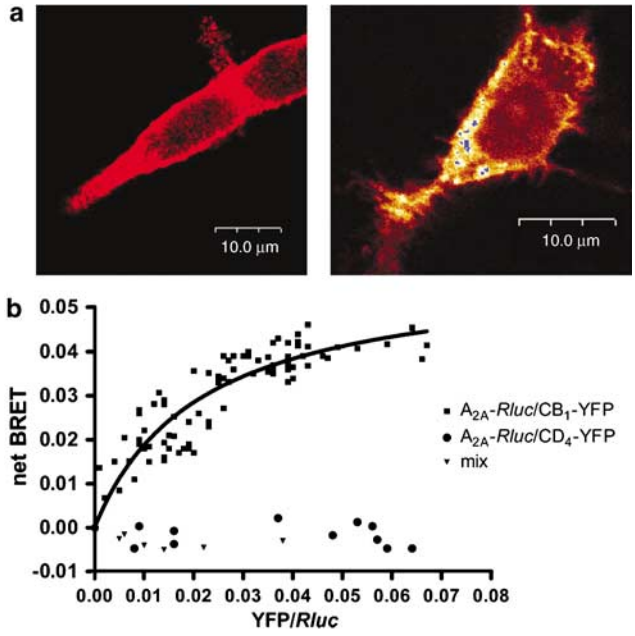

Figure 4 A_{2A}–CB_1 receptor heteromerization in living cells. HEK293 cells were transiently co-transfected with plasmids containing the human A_{2A} receptor fused to *Renilla luciferase* (A_{2A}-*Rluc*) and the human CB_1 receptor fused to yellow fluorescent protein (CB_1-YFP). (a) Confocal microscopy images of cells showing transfected A_{2A}-*Rluc* (left panel), identified by a monoclonal mouse anti-A_{2A} and cyanine-3 (red)-conjugated donkey anti-mouse IgG, and transfected CB_1-YFP (right panel), detected by its own fluorescence. (b) BRET was measured in HEK293 cells co-expressing A_{2A}-*Rluc* and CB_1-YFP (squares) or CD4-YFP (circles) or in a mixture of cells only transfected with A_{2A}-*Rluc* and cells only transfected with CB_1-YFP (triangles) as indicated in Materials and methods. Co-transfections were performed with increasing amounts of plasmid DNA for the YFP construct, whereas the DNA for the *Rluc* construct was maintained constant.

microscopy (Figure 5b). Confocal analysis revealed high colocalization of both receptors (white color in Figure 2b, right panel). By coupling to $G_{s\text{-}olf}$ proteins, A_{2A} receptors stimulate adenylyl-cyclase and induce cAMP accumulation (Kull *et al*, 1999). On the other hand, CB_1 receptors couple to $G_{i\text{-}o}$ proteins, and inhibit adenylyl cyclase (Bidaut-Russell *et al*, 1990; Felder *et al*, 1995; Hillard *et al*, 1999). Functional interaction between A_{2A} and CB_1 receptors were then assessed in cAMP accumulation experiments. Treatment of SH-SY5Y cells with the selective CB_1 receptor agonist ACEA counteracted the increase in cAMP levels induced by forskolin, but the effect of ACEA was not significant in the presence of the A_{2A} receptor antagonist ZM241385 (Figure 6). This demonstrates that under basal conditions, CB_1 receptors are negatively coupled to adenylate cyclase and suggests that coupling of CB_1 receptors to G_i requires previous or simultaneous activation of A_{2A} receptors. Previous studies have shown that SH-SY5Y cells release significant amounts of adenosine, which could provide the sufficient tonic activation of A_{2A} receptors required to enable CB_1 receptor function (Salim *et al*, 2000). In fact, when cAMP levels were determined in the presence of the enzyme ADA (2 UI/ml), which rapidly metabolizes released adenosine and prevents tonic activation of adenosine receptors (Salim *et al*, 2000), ACEA was unable to affect forskolin-induced increases in cAMP levels (Figure 7). The A_{2A} receptor agonist CGS 21680 substantially increased cAMP levels when SH-SY5Y cells where preincubated with ADA and this was prevented by treatment with the A_{2A} receptor antagonist ZM241385 or by ACEA (Figure 8). The reversal of the CGS21680-induced increase of cAMP by ACEA was counteracted by the CB_1 receptor antagonist AM251 (Figure 8). Altogether, these results indicate that in human neuroblastoma SH-SY5Y cells, activation of A_{2A} receptors is necessary for CB_1 receptor signaling.

Counteraction of Striatal CB_1 Receptor-Mediated Motor Depression by A_{2A} Receptor Antagonist

The *in vitro* biochemical studies described above predicted that A_{2A} receptor antagonists would reduce *in vivo* behavioral effects of CB_1 activation involving striatal function. To test this hypothesis, we studied the effects of blockade of A_{2A} receptors by a previous systemic administration of the potent and selective A_{2A} receptor antagonist MSX-3 on the motor effects induced by the bilateral striatal administration of the cannabinoid receptor agonist WIN 55 212-2. Here we show that the striatal administration of WIN 55 212-2 produces a significant motor depressant effect, both on locomotion and stereotypied behavior in nonhabituated rats (Figure 9). Although WIN 55 212-2 is a nonselective CB_1–CB_2 receptor agonist (Felder *et al*, 1995; Hillard *et al*, 1999), previous studies have shown that the motor depressant effects produced by systemic administration of WIN 55 212-2 are mediated by CB_1 receptors (Gifford *et al*, 1999; Darmani, 2001). Nevertheless, in the present behavioral model, the involvement of CB_1 receptors was demonstrated by the ability of two selective CB_1 receptor antagonists, SR141716A and AM251, to counteract the motor depression induced by the intrastriatal administration of WIN 55 212-2 (Figure 9). Importantly, previous systemic administration of MSX-3 did not by itself significantly modify motor activity in vehicle-treated animals, but it completely counteracted the motor depression produced by WIN 55 212-2, indicating that *in vivo* CB_1

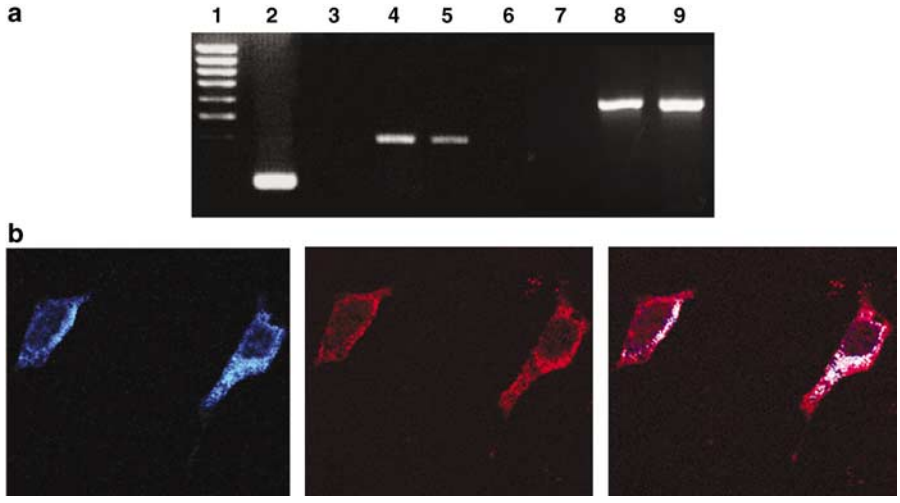

Figure 5 A_{2A} and CB_1 receptor expression in human neuroblastoma SH-SY5Y cells. (a) RT-PCR analysis of CB_1 and A_{2A} gene expression in SH-SY5Y cells. RT-PCR was performed using total RNA from SH-SY5Y cells (lanes 2, 5 and 9) or RNA from human striatum as positive control (lanes 4 and 8) and primers specific for the human CB_1 receptor gene (lanes 4 and 5), for the human A_{2A} receptor gene (lanes 8 and 9) or for tubulin (lane 2). Primers without cDNA (lanes 3 and 7) and RNA from SH-SY5Y with primers (lane 6) were included as negative controls. Molecular mass markers are shown in lane 1. (b) Immunocytochemical detection of CB_1 and A_{2A} receptors in SH-SY5Y cells were analyzed by confocal microscopy. Double-immunofluorescence staining was performed using cyanine 5(blue)-conjugated rabbit anti-CB_1 (left panel) and monoclonal mouse anti-A_{2A} antibodies detected with cyanine 3 (red)-conjugated donkey anti-mouse IgG (center panel). Superposition of images (right panel) reveals the colocalization of CB_1 and A_{2A} receptors in white.

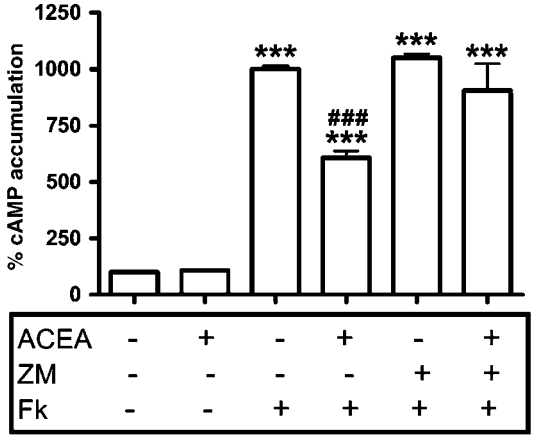

Figure 6 Functional interaction between A_{2A} and CB_1 receptors in human neuroblastoma SH-SY5Y cells. Accumulation of cAMP was measured in the presence or absence of 10 μM forskolin (Fk), 50 nM of the CB_1 receptor agonist ACEA, or 1 μM of the A_{2A} receptor antagonist ZM241385 (ZM), alone or in combination. Results are expressed as percentage of control (means ± SEM of 6–12 determinations from experiments performed in duplicate). *** and $^{###}P<0.0001$ compared to control and Fk alone, respectively (one-way ANOVA).

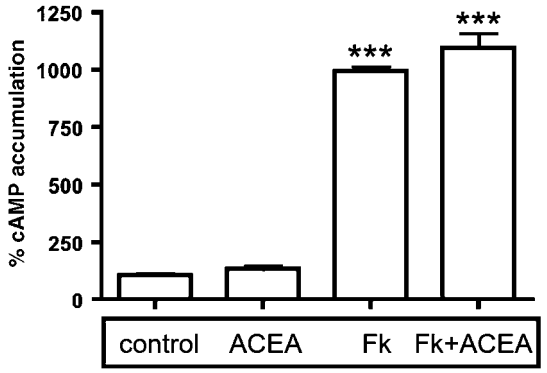

Figure 7 CB_1 receptor signalling in human neuroblastoma SH-SY5Y cells in the presence of ADA. Cells were treated overnight with 2 UI/ml of ADA and intracellular cAMP accumulation was measured in absence or presence of 10 μM forskolin (Fk) or 50 nM of the CB_1 receptor agonist ACEA, alone or in combination. Results are expressed as percentage of the control obtained in the absence of ligands (means ± SEM of 6–8 determinations from experiments performed in duplicate). ***$P<0.0001$ compared with control (one-way ANOVA).

receptor signaling that controls motor activity depends on A_{2A} receptor activation (Figure 9).

Binding of A_{2A} Receptor Antagonists to CB_1 Receptors

Although A_{2A} receptor antagonists behaved as CB_1 receptor antagonists in both *in vitro* and *in vivo* models, their ability to bind to the CB_1 receptor was not supported by radioligand binding experiments. No significant inhibition of the binding of a low concentration (0.1 nM) of [^{3}H]CP55 940 to rat striatal or cortical membranes was observed with 1 μM of ZM241385 (2 ± 3 and 4 ± 3, respectively), MSX-2 (6 ± 3 and 1 ± 1, respectively), or MSX-3 (9 ± 2 and 3 ± 6, respectively). In the same assay, CP55 940 displayed a K_i value of 0.83 ± 0.06 nM in striatal membranes.

DISCUSSION

It is becoming clear that the concept of heptaspanning G protein-coupled receptors (GPCRs) as single functional units has to be changed to a new concept that considers GPCRs as components of supramolecular aggregates, which include the same or other GPCRs, forming homomers or heteromers (Agnati *et al*, 2003, 2005; Franco *et al*, 2003, 2005). Heteromerization considerably increases the possible functional responses of GPCRs and its potential in drug discovery is just beginning to be considered (George *et al*,

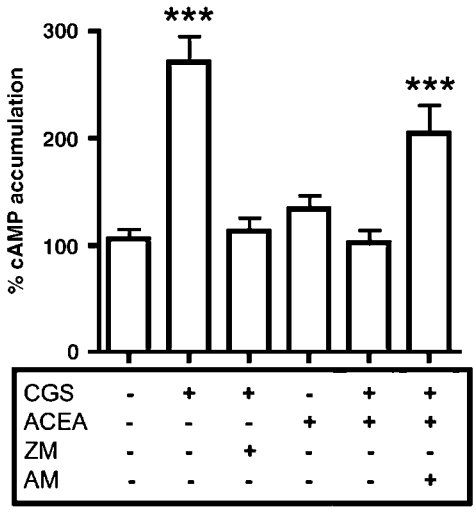

Figure 8 CB_1 and A_{2A} receptor signalling in human neuroblastoma SH-SY5Y cells in the presence of ADA. Cells were treated overnight with 2 UI/ml of ADA and intracellular cAMP accumulation was measured in absence or presence of 200 nM of the A_{2A} receptor agonist CGS21680 (CGS), 50 nM of the CB_1 receptor agonist ACEA (ACEA), 1 μM of the A_{2A} receptor antagonist ZM241385 (ZM), or 1 μM of the CB_1 receptor antagonist AM251 (AM), alone or in combination. Results are expressed as percentage of the control obtained in the absence of ligands (means ± SEM of 6–8 determinations from experiments performed in duplicate). ***$P < 0.0001$ compared to control (one-way ANOVA).

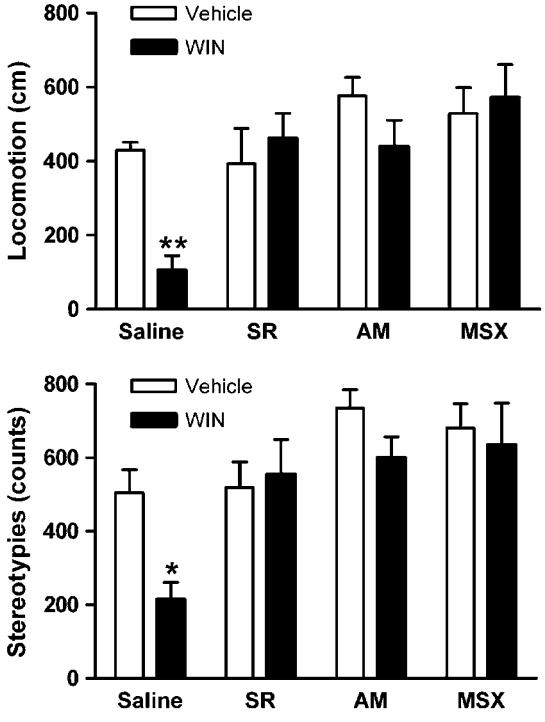

Figure 9 Functional interaction between A_{2A} and CB_1 receptors in the rat striatum. The CB1 receptor antagonists SR141716A (SR; 3 mg/kg i.p.) and AM251 (AM; 3 mg/kg i.p.) and the A_{2A} receptor antagonist MSX-3 (MSX; 3 mg/kg i.p.) or saline (S) were administered systemically 20 min before the intrastriatal bilateral administration of the cannabinoid receptor agonist WIN 55 212-2 (WIN; 40 μg/side) or its vehicle. Motor activity, locomotion and stereotypies were recorded 20 min after WIN 55 212-2 administration. Results are expressed as means ± SEM ($n = 5$–7/group) of the average of the motor activity recordings obtained during the first four 5-min intervals. * and **$P < 0.05$ and $P < 0.01$ compared to the control group (saline-vehicle; one-way ANOVA).

2002; Maggio *et al*, 2005). By means of *in vitro* and *in vivo* approaches, we now demonstrate that both physical and functional interactions between striatal A_{2A} and CB_1 receptors exist and that these interactions play a significant role in the motor depressant effects of CB_1 receptor agonists.

Adenosine A_{2A} receptors are most abundant in the striatum, where they are preferentially localized in the dendritic spines of the striatopallidal GABAergic enkephalinergic neurons and also presynaptically in glutamatergic terminals (Hettinger *et al*, 2001; Ciruela *et al*, 2006). Striatal CB_1 receptors are located in the dendritic spines of GABAergic neurons, including the striatopallidal neurons, and they are also located on nerve terminals (Rodriguez *et al*, 2001; Kofalvi *et al*, 2005; Julian *et al*, 2003). By using immunofluorescent histochemical techniques, we demonstrated that A_{2A} and CB_1 receptors are in fact colocalized in the same striatal elements, in fibrilar structures, which represent either dendritic processes or nerve terminals. A yellow fluorescent signal showed colocalization of CB_1 and A_{2A} receptors in approximately half of the total fibers expressing CB_1 receptors, and the absence of a red immunoreactive signal in the merged images indicates that most A_{2A} receptors are colocalized with CB_1 receptors (Figure 2c, f, and i). This agrees with the more widespread localization of striatal CB_1 receptors (see Introduction). These results provide the anatomical basis needed to sustain A_{2A}–CB_1 receptor interactions in the striatum. We first demonstrate the existence of A_{2A}–CB_1 heteromeric receptor complexes in rat striatal membranes by co-immunoprecipitation. We then show that A_{2A} and CB_1 receptors can form 'true heteromers' using BRET in HEK-293T living cells. These physical interactions suggested a functional interdependence between A_{2A} and CB_1 receptors. Such a functional interdependence is demonstrated by our findings that both CB_1 receptor signaling in a human neuroblastoma cell line and the motor depressant effects of CB_1 receptor agonists in rats are dependent on A_{2A} receptor activation.

In recent studies, some biochemical effects of CB_1 receptor agonists have been reported to depend on A_{2A} receptor function, although it was suggested that these effects might be due to indirect interactions involving dopamine D_2 receptors (Yao *et al*, 2003; Andersson *et al*, 2005). In the present study, we found a functional A_{2A}–CB_1 receptor interdependence in cells (human neuroblastoma SH-SY5Y cell line) that do not express D_2 receptors. In those cells, CB_1 receptor stimulation could only produce a decrease in cAMP levels if A_{2A} receptors were simultaneously co-activated. This indicates that activation of A_{2A} receptors in the CB_1–A_{2A} receptor heteromer allows the effective coupling of CB_1 receptor to G_i proteins. It must however be pointed out that Soria *et al* (2004) found that the genetic activation of A_{2A} receptors did not impair the ability of cannabinoid agonists to activate G_i proteins. Similarly, previous studies in transfected cells have also shown that CB_1 receptors couple and activate G_i proteins (CB_1 receptor agonist-induced inhibition of forskolin-induced cAMP accumulation) in the absence of A_{2A} receptors (Felder *et al*, 1995; Hillard *et al*, 1999). Therefore, our results strongly suggest that it is in the presence of A_{2A} receptors (when forming A_{2A}–CB_1 receptor heteromers) that CB_1 receptor function depends on A_{2A} receptor

activation. The results, however, do not discard the existence of G_i-independent signal-transduction pathways that do not depend on A_{2A} receptor function. In fact, several studies suggest that CB_1 receptors can also couple to G_s under some conditions (for review, see Demuth and Molleman, 2006). Furthermore, we cannot discard the possibility that functional A_{2A}–CB_1 receptor interactions could take place with the receptors being close enough but not physically (directly or indirectly) connected.

It is generally accepted that the basal ganglia are the main brain areas involved in the motor depressant effects of cannabinoids and CB_1 receptor agonists (Gough and Olley, 1978; Sanudo-Pena *et al*, 1999; van der Stelt and Di Marzo, 2003). However, there is no consensus about the role played by the different structures of the basal ganglia, with some authors giving more relevance to the striatum and others to projecting striatal areas (globus pallidus and substantia nigra pars reticulata) (Gough and Olley, 1978; Sanudo-Pena *et al*, 1999; van der Stelt and Di Marzo, 2003). The present study indicates an important role for the striatum, as a pronounced depression of exploratory activity was observed with the intrastriatal administration of the cannabinoid receptor agonist WIN 55 212-2, which was counteracted by the systemic administration of CB_1 receptor antagonists. Furthermore, the motor depressant effect of WIN 55 212-3 was completely counteracted by previous systemic administration of the selective A_{2A} receptor antagonist MSX-3. Importantly, these results provide an *in vivo* behavioral correlate for the biochemical results obtained with the neuroblastoma cell line, indicating that some functional effects of striatal CB_1 receptors effects depend on A_{2A} receptor function. The inability of A_{2A} receptor antagonists to bind to the CB_1 receptor shown in the present radioligand binding experiment indicates that the CB_1-receptor-antagonist-like behavior of A_{2A} receptor antagonists is due to a functional A_{2A}–CB_1 receptor interdependence. It has recently been shown that genetic and also pharmacological blockade of A_{2A} receptors significantly, but only partially, reduces cataleptogenic effects induced by systemic administration of the CB_1 receptor agonist CP55 940 (Andersson *et al*, 2005). On the other hand, Soria *et al* (2004) reported a lack of changes in the motor depressant effects induced by the systemic administration of THC in A_{2A} receptor knockout mice. Our results demonstrate that a selective A_{2A} receptor antagonist can completely counteract the motor depression produced by the striatal activation of CB_1 receptors, suggesting that motor-depressant effects of systemically administered CB_1 receptor agonists depend on both striatal (A_{2A} receptor-dependent) and nonstriatal (A_{2A} receptor-independent) CB_1 receptors. Soria *et al* (2004) also reported a decreased place preference to THC in mice with genetic blockade of A_{2A} receptors. This further suggests that the rewarding effects of cannabinoids might also depend on striatal A_{2A}–CB_1 receptor heteromeric complexes, although the main anatomical target for those effects is still a matter of debate.

ACKNOWLEDGEMENTS

This research was supported in part by grants from Spanish Ministerio de Ciencia y Tecnología (SAF2005-00903 to FC and SAF2005-00170 to EIC and SAF2003-04864 and PNSD to RM) and in part by the Intramural Research Program of the National Institutes of Health.

REFERENCES

Andersson M, Usiello A, Borgkvist A, Pozzi L, Dominguez C, Fienberg AA *et al* (2005). Cannabinoid action depends on phosphorylation of dopamine- and cAMP-regulated phosphoprotein of 32 kDa at the protein kinase A site in striatal projection neurons. *J Neurosci* **25**: 8432–8438.

Agnati LF, Ferré S, Lluis C, Franco R, Fuxe K (2003). Molecular mechanisms and therapeutical implications of intramembrane receptor/receptor interactions among heptahelical receptors with examples from the striatopallidal GABA neurons. *Pharmacol Rev* **55**: 509–550.

Agnati LF, Fuxe K, Ferré S (2005). How receptor mosaics decode transmitter signals. Possible relevance of cooperativity. *Trends Biochem Sci* **30**: 188–193.

Bidaut-Russell M, Devane WA, Howlett AC (1990). Cannabinoid receptors and modulation of cyclic AMP accumulation in the rat brain. *J Neurochem* **55**: 21–26.

Chen JF, Huang Z, Ma J, Zhu J, Moratalla R, Standaert D *et al* (1999). A(2A) adenosine receptor deficiency attenuates brain injury induced by transient focal ischemia in mice. *J Neurosci* **19**: 9192–9200.

Ciruela F, Casado V, Rodrigues RJ, Lujan R, Burgueno J, Canals M *et al* (2006). Presynaptic control of striatal glutamatergic neurotransmission by adenosine A1-A2A receptor heteromers. *J Neurosci* **26**: 2080–2087.

Cunha RA, Constantino MD, Ribeiro JA (1997). ZM241385 is an antagonist of the facilitatory responses produced by the A2A adenosine receptor agonists CGS21680 and HENECA in the rat hippocampus. *Br J Pharmacol* **122**: 1279–1284.

Darmani NA (2001). Delta(9)-tetrahydrocannabinol and synthetic cannabinoids prevent emesis produced by the cannabinoid CB(1) receptor antagonist/inverse agonist SR 141716A. *Neuropsychopharmacology* **24**: 198–203.

Demuth DG, Molleman A (2006). Cannabinoid signalling. *Life Sci* **78**: 549–563.

Felder CC, Joyce KE, Briley EM, Mansouri J, Mackie K, Blond O *et al* (1995). Comparison of the pharmacology and signal transduction of the human cannabinoid CB1 and CB2 receptors. *Mol Pharmacol* **48**: 443–450.

Ferré S, Borycz J, Goldberg SR, Hope BT, Morales M, Lluis C *et al* (2005). Role of adenosine in the control of homosynaptic plasticity in striatal excitatory synapses. *J Integr Neurosci* **4**: 445–464.

Ferré S, Fredholm BB, Morelli M, Popoli P, Fuxe K (1997). Adenosine-dopamine receptor–receptor interactions as an integrative mechanism in the basal ganglia. *Trends Neurosci* **20**: 482–487.

Franco R, Canals M, Marcellino D, Ferré S, Agnati L, Mallol J *et al* (2003). Regulation of heptaspanning-membrane-receptor function by dimerization and clustering. *Trends Biochem Sci* **28**: 238–243.

Franco R, Casado V, Mallol J, Ferré S, Fuxe K, Cortes A *et al* (2005). Dimer-based model for heptaspanning membrane receptors. *Trends Biochem Sci* **30**: 360–366.

Fusco FR, Martorana A, Giampa C, De March Z, Farini D, D'Angelo V *et al* (2004). Immunolocalization of CB1 receptor in rat striatal neurons: a confocal microscopy study. *Synapse* **53**: 159–167.

George SR, O'Dowd BF, Lee SP (2002). G-protein-coupled receptor oligomerization and its potential for drug discovery. *Nat Rev Drug Discov* **1**: 808–820.

Gerfen CR (2004). Basal Ganglia. In: Paxinos G (ed). *The Rat Nervous System*. Elsevier Academic Press: Amsterdam. pp 445–508.

Gifford AN, Bruneus M, Gatley SJ, Lan R, Makriyannis A, Volkow ND (1999). Large receptor reserve for cannabinoid actions in the central nervous system. *J Pharmacol Exp Ther* **288**: 478–483.

Gough AL, Olley JE (1978). Catalepsy induced by intrastriatal injections of delta9-THC and 11-OH-delta9-THC in the rat. *Neuropharmacology* **17**: 137–144.

Herkenham M, Lynn AB, de Costa BR, Richfield EK (1991). Neuronal localization of cannabinoid receptors in the basal ganglia of the rat. *Brain Res* **547**: 267–274.

Hettinger BD, Lee A, Linden J, Rosin DL (2001). Ultrastructural localization of adenosine A2A receptors suggests multiple cellular sites for modulation of GABAergic neurons in rat striatum. *J Comp Neurol* **431**: 331–346.

Hillard CJ, Manna S, Greenberg MJ, DiCamelli R, Ross RA, Stevenson LA *et al* (1999). Synthesis and characterization of potent and selective agonists of the neuronal cannabinoid receptor (CB1). *J Pharmacol Exp Ther* **289**: 1427–1433.

Hillion J, Canals M, Torvinen M, Casado V, Scott R, Terasmaa A *et al* (2001). Coaggregation, cointernalization, and codesensitization of adenosine A2A receptors and dopamine D2 receptors. *J Biol Chem* **277**: 18091–18097.

Hohmann AG, Herkenham M (2000). Localization of cannabinoid CB(1) receptor mRNA in neuronal subpopulations of rat striatum: a double-label *in situ* hybridization study. *Synapse* **37**: 71–80.

Howlett AC, Song C, Berglund BA, Wilken GH, Pigg JJ (1998). Characterization of CB1 cannabinoid receptors using receptor peptide fragments and site-directed antibodies. *Mol Pharmacol* **53**: 504–510.

Julian MD, Martin AB, Cuellar B, Rodriguez De Fonseca F, Navarro M, Moratalla R *et al* (2003). Neuroanatomical relationship between type 1 cannabinoid receptors and dopaminergic systems in the rat basal ganglia. *Neuroscience* **119**: 309–318.

Karcz-Kubicha M, Antoniou K, Terasmaa A, Quarta D, Solinas M, Justinova Z *et al* (2003). Involvement of adenosine A1 and A2A receptors in the motor effects of caffeine after its acute and chronic administration. *Neuropsychopharmacology* **28**: 1281–1291.

Klegeris A, Bissonnette CJ, McGeer PL (2003). Reduction of human monocytic cell neurotoxicity and cytokine secretion by ligands of the cannabinoid-type CB2 receptor. *Br J Pharmacol* **139**: 775–786.

Kofalvi A, Rodrigues RJ, Ledent C, Mackie K, Vizi ES, Cunha RA *et al* (2005). Involvement of cannabinoid receptors in the regulation of neurotransmitter release in the rodent striatum: a combined immunochemical and pharmacological analysis. *J Neurosci* **25**: 2874–2884.

Kull B, Ferré S, Arslan G, Svenningsson P, Fuxe K, Owman C *et al* (1999). Reciprocal interactions between adenosine A2A and dopamine D2 receptors in Chinese hamster ovary cells co-transfected with the two receptors. *Biochem Pharmacol* **58**: 1035–1045.

Lan R, Liu Q, Fan P, Lin S, Fernando SR, McCallion D *et al* (1999). Structure–activity relationships of pyrazole derivatives as cannabinoid receptor antagonists. *J Med Chem* **42**: 769–776.

Ledent C, Valverde O, Cossu G, Petitet F, Aubert JF, Beslot F *et al* (1999). Unresponsiveness to cannabinoids and reduced addictive effects of opiates in CB1 receptor knockout mice. *Science* **283**: 401–404.

Maggio R, Novi F, Scarselli M, Corsini GU (2005). The impact of G-protein-coupled receptor hetero-oligomerization on function and pharmacology. *FEBS J* **272**: 2939–2946.

Sanudo-Pena MC, Tsou K, Walker JM (1999). Motor actions of cannabinoids in the basal ganglia output nuclei. *Life Sci* **65**: 703–713.

Rodriguez JJ, Mackie K, Pickel VM (2001). Ultrastructural localization of the CB1 cannabinoid receptor in mu-opioid receptor patches of the rat caudate putamen nucleus. *J Neurosci* **21**: 823–833.

Salim H, Ferré S, Dalal A, Peterfreund RA, Fuxe K, Vincent JD *et al* (2000). Activation of adenosine A1 and A2A receptors modulates dopamine D2 receptor-induced responses in stably transfected human neuroblastoma cells. *J Neurochem* **74**: 432–439.

Sauer R, Maurinsh J, Reith U, Fulle F, Klotz KN, Muller CE (2000). Water-soluble phosphate prodrugs of 1-propargyl-8-styrylxanthine derivatives, A(2A)-selective adenosine receptor antagonists. *J Med Chem* **43**: 440–448.

Soria G, Castane A, Berrendero F, Ledent C, Parmentier M, Maldonado R *et al* (2004). Adenosine A2A receptors are involved in physical dependence and place conditioning induced by THC. *Eur J Neurosci* **20**: 2203–2213.

Twitchell W, Brown S, Mackie K (1997). Cannabinoids inhibit N- and P/Q-type calcium channels in cultured rat hippocampal neurons. *J Neurophysiol* **78**: 43–50.

van der Stelt M, Di Marzo V (2003). The endocannabinoid system in the basal ganglia and in the mesolimbic reward system: implications for neurological and psychiatric disorders. *Eur J Pharmacol* **480**: 133–150.

Yao L, Fan P, Jiang Z, Mailliard WS, Gordon AS, Diamond I (2003). Addicting drugs utilize a synergistic molecular mechanism in common requiring adenosine and Gi-beta gamma dimers. *Proc Natl Acad Sci USA* **100**: 14379–14384.